Supporting Information for

Well-Controlled Formation of Polymeric Micelles with a Nano-Sized Aqueous Core and their Applications as Nanoreactors

Fei Cheng,[†] Xiaogang Yang, [†] Huisheng Peng, [‡] Daoyong Chen, *,[†] and Ming Jiang[†]

[†] *Key Laboratory of Molecular Engineering of Polymers of Ministry of Education, Department of Macromolecular Science, Fudan University, Shanghai 200433, China*
[‡] *Los Alamos National Laboratory, Los Alamos, NM 87545, USA*

S1. TEM images of the aggregates formed at the *transfer time* (*t*) of 0 and 1 minute.

From Figure S1a, we can see that no regular aggregate was formed at *t*=0 min since the block copolymer was molecularly dispersed in its common solvent chloroform before the protonation of the P4VP block chains.

From Figure S1b, we can see that the aggregates formed at *t*=1 min are polydispersed. The diameter of the aggregates observed by TEM was much smaller than that measured by DLS ($<D_h>$=306 nm, Figure1), indicating the remarkable shrinking of the aggregates on copper grid during sample drying. This is consistent with the loosely aggregated structure of the aggregates formed at t=1 min, indicated by the very low intensity of the scattering light of the aggregates solution (mentioned in the main text). The irregular particles with a relatively low contrast in Figure S1b, which can be discerned on the background of the TEM image, may result from the molecularly dispersed block copolymer chains in the solution, which then aggregate together during the TEM sample drying. The morphology of the aggregates in Figure S1b shows the characteristics of the aggregates formed by anomalous micellization.
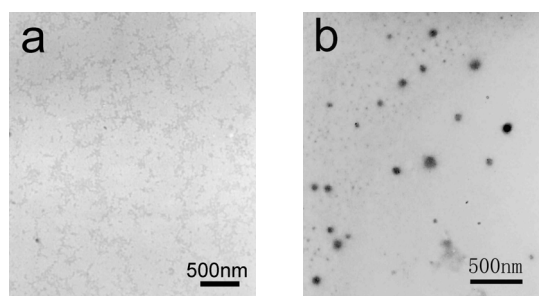
Figure S1. TEM images of micelles formed at transfer time of 0 (a) and 1 (b) minute.

S2. ^{1}H NMR spectrum of pH 1 HCl-saturated CDCl$_3$.

10 mL of pH 1 HCl aqueous solution was added carefully to the top of deuterated chloroform phase (1mL CDCl$_3$). Then the biphase system was gently magnetically stirred for more than 5 days. Afterwards, the bottom CDCl$_3$ was taken out and characterized by ^{1}H NMR. The molecularly dispersed water molecules in CDCl$_3$ give a sharp peak at 1.59 ppm (Figure S2). Because the biphase system was gently stirred by a small magnetic bar in CDCl$_3$ phase, no water droplets can diffuse into CDCl$_3$. Besides, without any stabilizer, water droplets, which should present a signal at 4~5 ppm in the ^{1}H NMR spectrum (based on the ^{1}H NMR result of S3 and the results obtained by Eisenberg et al. *Macromolecules* **1992,** 25, (4), 1300-1303), cannot be stabilized in CDCl$_3$. Therefore, we are inclined to attribute the small peak at 3.5 ppm to the HCl molecules, which are expected to be unionized in such a low-polarity medium (a small amount in CDCl$_3$. Please also refer to S3).
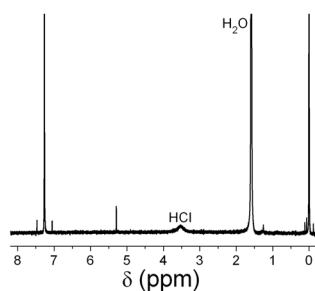

Figure S2. ^{1}H NMR spectrum of pH 1 HCl saturated CDCl$_3$

S3. ^{1}H NMR spectra of H$_2$O and H$_2$O+HCl in D$_2$O.

The mixture of 0.05 mL deioned water in 0.5 mL D$_2$O and that of 0.05 mL of 38% (w/w) HCl aqueous solution in 0.5 mL D$_2$O were characterized by ^{1}H NMR, respectively. This control experiment was conducted to confirm that water droplets (in which individual water molecules are dispersed in a medium constructed by water) will give signals at 4~5 ppm. From Figure S3 we can see that, H$_2$O molecules in an environment formed by D$_2$O, which is comparable to H$_2$O molecules in a water droplet, present a signal at 4.68 ppm. When coexisting with HCl, the H$_2$O signal shifts to a low field (4.78 ppm). These support our conclusions made in S2: no water droplets exist in chloroform phase; the small peak appearing at 3.5 ppm should be

attributed to HCl molecules in CDCl$_3$.

The sharp peak d' at ~4.8 ppm in spectra I~K of Figure 2a shows similar characteristics to the peaks seen in Figure S3, so it should be attributed to the free water existing in the polar and acidic core of the PMACs.
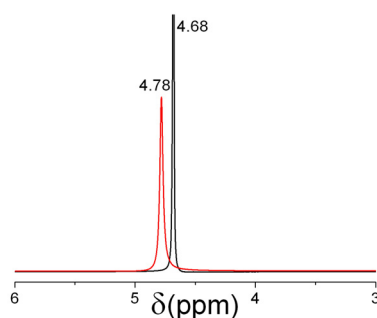
Figure S3. ^{1}H NMR spectrum of H$_2$O (black) and H$_2$O/HCl (red) in D$_2$O.

S4. The explanation of "bound water", "intermediate water" and "free water".

The definition of "three-state" water was given in the paper Biomacromolecules; 2002; 3(5); 991-997. According to the definition, "bound water" can behave dynamically and thermodynamically as part of the polymer chains when the water molecules interact strongly with specific sites; "free" or "bulklike" water molecules are those whose interaction with the polymer chains is negligible; "intermediate" water molecules interact with the polymer chains weakly. In the present study, the "bound water" should be aggregated together with protonated P4VP chains so that they could not be detected by liquid ^{1}H NMR at early stage of micellization (t≤15 min); the "free" or "bulklike" water gave sharp peaks in the ^{1}H NMR spectra; the water molecules giving the wide peaks in spectra were attributed to the intermediate water. These intermediate water molecules interact with the polymer chains as evidenced by the remarkable widening of their signals in the liquid ^{1}H NMR spectra, but the interaction is weak so that they are detectable in liquid ^{1}H NMR spectra.

S5. The calculation of water content in the cores of micelles at different *t*.

We can't evaluate the molar ratios and mass ratios of the water to the 4-vinylpyridine (4VP) repeating units in the cores directly from the intensity ratios

between the respective peaks in the ^{1}H NMR spectra, because the intensities of the pyridine signals vary with the protonation and the micellization, as mentioned in the main text. However, the PS blocks are solubilized during the whole process and the intensities of the PS signals should be unchanged and proportional to the amount of the styrene repeating units in the solution. Therefore, the molar ratios and the mass ratios of the water to the benzene rings in the PMACs formed at a certain t can be evaluated based on the intensity ratio of peak d/peak b_1 in the spectra (when 40 min $\leq t \leq$ 10 hours) or (peak d + peak d')/peak b_1 (when $t \geq$ 24 hours). The mass ratios (M_1) and the molar ratios (M_2) of the water to the 4VP repeating units can thus be derived since those of the 4VP repeating units to the benzene rings are determined by the composition of the block copolymer. The formulae for calculating M_1 and M_2 are derived as below:

The molar ratio of water molecules to the styrene repeating units of the block copolymer $\dfrac{n_{water}}{n_{styrene}}$ should be:

$$\frac{n_{water}}{n_{styrene}} = \frac{A_{water}}{2} : \frac{A_{styrene}}{3} \qquad (1)$$

where A_{water} represents the area of peak d or peak d + peak d' and 2 is the number of H_d in a water molecule; $A_{styrene}$ represents the area of peak b_1 in a spectrum measured at a certain t (Figure 2, in main text) and 3 is the number of H_b atoms in a styrene repeating unit (Scheme 1, main text).

As PS$_{197}$-b-P4VP$_{343}$ was used for the present study, the molar ratio between the styrene repeating units and 4VP repeating units is 197/343. So:

$$M_2 = \frac{n_{water}}{n_{styrene}} \times \frac{197}{343} \qquad (2)$$

Putting (1) into (2), we get

$$M_2 = \frac{A_{water}}{A_{styrene}} \times 0.8615 \qquad (3)$$

M_1 can be calculated with

4

$$M_1 = M_2 \times \frac{18}{105} = \frac{A_{water}}{A_{styrene}} \times 0.1477 \qquad (4)$$

where 18 and 105 are the molecular weights of water molecules and 4-vinylpyridine repeating units, respectively.

S6. Discussion on the ^{1}H NMR signal of unprotonated pyridine units at t<10 hours.

In the article, we think that the ^{1}H NMR signal of unprotonated pyridine units at 10 hours > t ≥ 3 min is related to the unprotonated pyridine units existing in the swollen cores of micelles. This speculation is based on the fact that, when t≥3 min, our TEM observations find no irregular aggregates resulting from the molecularly solubilized block copolymer chains. Such irregular aggregates were observed in the system at t=1 min (Figure S1b), which are thought to be caused by the aggregation between the molecularly dispersed block copolymer chains during the solvent evaporation on the copper grid.

Ikalla et al. stated that the hydrogen bonding between P4VP and 3-pentadecylphenol in chloroform is irreversible (Ruokolainen, J.; tenBrinke, G.; Ikkala, O.; Torkkeli, M.; Serimaa, R. *Macromolecules* **1996**, *29*, 3409). Therefore, it is reasonable to think that the protonation of the pyridine units of the P4VP blocks in chloroform is also irreversible as the pKa of HCl in chloroform is much lower than that of 3-pentadecylphenol. Due to the irreversibility, the protonation is determined by the diffusion of HCl molecules as well as the diffusion of the block copolymer chains in CDCl$_3$. Therefore, the protonated pyridine units must be randomly distributed among unprotonated ones in all polymer chains. Based on this consideration, we believe that the possibility that some of the block copolymer chains that are almost un-protonated and molecularly solubilized in the chloroform phase is ignorable.

S7. The control experiment to stabilize water-in-chloroform reverse microemulsion with PS$_{197}$-b-P4VP$_{343}$ as the polymeric surfactant.

The experimental conditions are: 2.0 mL of block copolymer solution in chloroform at 2.0 mg/mL was mixed with 1.0 mL of pH1 HCl aqueous solution in a columnar vial under ultrasonic or vigorous stirring for 10 minutes at ambient temperature (~20°C). Then the mixtures were stood still, and the water and chloroform were phase separated after the standing for minutes. In both the cases, the top aqueous phase and the bottom chloroform phase were turbid. Besides, some precipitate appeared in the bottom chloroform phase. In the system mixed under ultrasonic, we discarded the aqueous phase and filtered out the precipitate in chloroform phase. Then the turbid chloroform solution was characterized with DLS. The $<D_h>$ is 522 nm, and the polydispersity index is 1.0.

S8. The effect of HCl on the transfer of inorganic species through chloroform phase.

We designed simple experiments to demonstrate that the transfer of inorganic compounds from the top aqueous phase through chloroform can be accelerated by HCl. In Figure 5a of the main text, a piece of filter paper soaked with $FeCl_3$ aqueous solution was placed at the bottom of vials *a1* and *a2* and covered by a 2 cm thick chloroform layer, respectively. Then, aqueous solution of NH_4SCN at 20.0 mg/mL in pH1 HCl and that in neutral deioned water were added to form the top aqueous phase in vials *a1* and *a2*, respectively. In Figure 5b (the main text), the bottom phase is also chloroform and the upper aqueous phase in vials *b1* and *b2* is the aqueous solution of $(NH_4)_2S_2O_8$ at 20.0 mg/mL in pH1 HCl and that in neutral deioned water, respectively. After the formation of biphase systems, the vials were set still. All experiments were conducted at ambient temperature (~20 °C).

S9. The EDX analysis of $Fe^{3+}/(SCN)^-$ nanoparticles formed in PMACs.

The components encapsulated in the cores of PMACs (see Figure 6 in the main text) were analyzed by EDX (energy-dispersive X-ray spectroscopy) focused on the particles. 0.1 ml of the solution (or dispersion system) of the $Fe^{3+}/(SCN)^-$/PMACs composite nanoparticles in chloroform was dropped and dried on a piece of fresh

cleaved mica, whose area is 1cmX1cm. Then the sample was characterized on a PHILIPS XL30 scanning electron microscope. Averaged over ten EDX measurements, the average number ratio of S atoms to Fe atoms was determined to be 1/14. Figure S4 is a typical EDX spectrum of the composite nanoparticles.
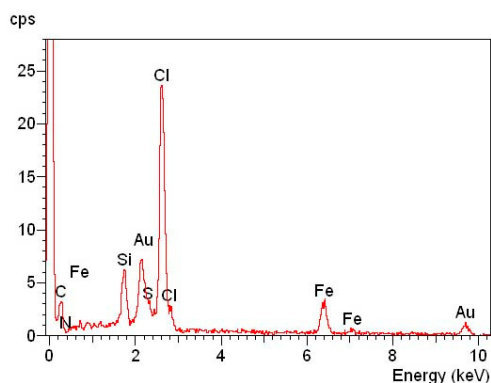

Figure S4. EDX spectrum of $Fe^{3+}/(SCN)^-/PMACs$ composite nanoparticles.

Considering the facts that Fe is largely excessive and there is an equilibrium between the complexes formed by Fe^{3+} and SCN^{-1}: $Fe(SCN)_3 \rightleftharpoons Fe(SCN)^{2+} + 2SCN^{-1}$, where $Fe(SCN)^{2+}$ is red (The Important Inorganic Reactions, 2nd Edition, Shouchun Chen, Shanghai Science and Technology Press, 1982). Therefore, we believe that the complex formed in the core with a red color should mainly be the $Fe(SCN)^{2+}$.

S10. Using PMACs as nanoreactors with solid FeCl₃ and NH₄SCN as precursors.

We also successfully loaded $FeCl_3$ solid and NH_4SCN solid into PMACs at the same time. This experiment was conducted at ambient temperature (~20 °C). At the beginning of the experiment, 10.0 mg of $FeCl_3$ solid was placed on the bottom of vial 1 and 10.0 mg of NH_4SCN solid on the bottom of vial 2. Vial 1 and vial 2 are connected by a channel (Figure S5). Then 6.0 mL of PMACs solution at the concentration of the block copolymer of 2.0 mg/mL was added. The color of PMACs solution turned to dark red in hours (Figure S5). We have demonstrated that without PMACs, the chloroform phase saturated with water and HCl cannot host the reaction between Fe^{3+} and SCN^{-1}. Therefore, the red color formed in the H-shaped tube

demonstrates that $FeCl_3$ and NH_4SCN were loaded into PMACs although the precursors are in solid state. The two precursors reacted in the aqueous cores of the PMACs, forming $Fe(SCN)^{2+}$.
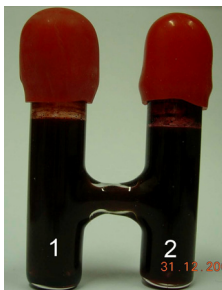
**Figure S5.** Digital picture of PMAC nanoreactors for preparing $Fe(SCN)^{2+}$ with solid $FeCl_3$ and NH_4SCN as precursors.

S11. Calculating the mass ratio of Ag to Ag_2ClNO_3 in Figure 8.

We calculated the mass ratio of Ag to Ag_2ClNO_3 according to the XRD pattern of the composite particles (Figure 8b) based on the absolute XRD diffraction intensities of Ag and Ag_2ClNO_3 (See **Mater, Res, Soc, Symp, Proc 2005, 865E, BB2,3,1-BB2,3,6**). The procedures are:

First, we modeled the XRD patterns of pure Ag and Ag_2ClNO_3 crystals with software **PowerCell Version 2.4**. The parameters used for the modeling were obtained from **JCPDS cards, No. 89-3722; JCPDS cards, No. 70-2186**, and *Acta Crystallographica Section B* **1979, 35, 1432-1435**. The modeled Crystal structures and XRD patterns were give in Figure S6.
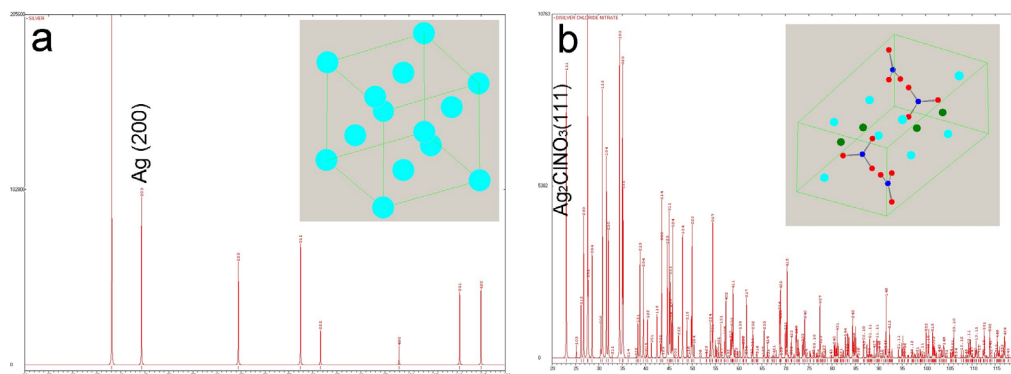
Figure S6. The modeled XRD patterns of pure Ag (a) and Ag_2ClNO_3 (b) crystals.

Then we choose peak Ag (200) with the calculated absolute intensity of 98903 and peak Ag_2ClNO_3 (111) with the absolute intensity of 8989 to calculate the mass ratio of Ag/Ag_2ClNO_3.

$$R = \frac{I_{Ag(200),exp} / I_{Ag(200), calculated}}{I_{Ag_2ClNO_3(111),exp} / I_{Ag_2ClNO_3(111), calculated}} \times 100\%$$

where R is the mass ratio of Ag/Ag_2ClNO_3; $I_{Ag(200),exp}$ and $I_{Ag_2ClNO_3(111),exp}$ are the intensities of peak Ag (200) and peak Ag_2ClNO_3 (111) in Figure 8b, respectively (the intensities of the peaks were calculated with software **PeakFit Version 4.12**); $I_{Ag(200), calculated}$ and $I_{Ag_2ClNO_3(111), calculated}$ are the absolute intensities of peak Ag (200) and peak Ag_2ClNO_3 (111) read from the modeled XRD patterns in Figure S6, respectively.

Putting $I_{Ag(200),exp} = 7.48$, $I_{Ag(200), calculated} = 98903$, $I_{Ag_2ClNO_3(111),exp} = 66.51$ and $I_{Ag_2ClNO_3(111), calculated} = 8989$ into (1), we get:

R=1.02 %.

This result indicates that the mass ratio of byproduct Ag to Ag_2ClNO_3 in the resultant composite nanoparticles is quite low.